

1

p-toluenesulfonic acid at 200 °C. The resulting bis(imidazole) was oxidized with BaMnO₄ according to the procedure we developed for 2-substituted imidazoles,²⁷ and **1** was isolated as colorless crystals, mp 273–274 °C.²⁸ Complexes of **1** were prepared by treatment with 0.5 equiv of the M(II) perchlorate in ethanol. The green Cu(II) complex (1.7 μ_B) crystallized as the diperchlorate from acetone–ether. The dark-blue Ni(II) (3.7 μ_B), purple Co(II), (4.7 μ_B), and colorless Zn(II) complexes crystallized from ethanol–ether as isostructural diperchlorates having three lattice ethanol molecules per metal. The Cu(I) complex was obtained as the pale-yellow perchlorate by diffusing ether into a deoxygenated acetonitrile solution containing 1 equiv of **1** and 0.5 equiv of Cu(CH₃CN)₄·ClO₄.

From X-ray analysis, the metal ions were found to lie on twofold axes which either relate two molecules of **1** in the 2:1 complexes (Ni(II), Co(II), Zn(II), Cu(I)), or which bisect the biphenyl 1,1'-bond and relate halves of **1** [Cu(I), Cu(II), Figures 1 and 2].²⁹ Comparison of the figures shows the strong similarity of the Cu(I) and Cu(II) structures. Geometrical constraints within the nine-membered chelate rings cause the intraligand N(1)–M–N(1') angles to exceed 109°, flattening the otherwise tetrahedral MN₄ units. Additional LF effects result in larger angles for the Cu(II) [140.3 (4)°, 142.5 (4)°] and Ni(II) [130.2 (2)°] complexes compared with those for Co(II) [123.2 (2)°] and Cu(I) [119.5 (3)°, 121.6 (3)°]. The DA's between the intraligand N₂M units (e.g., N(1)–M–N(1')/N(3)–M–N(3'), Figure 1) are 86.4 (2)°, 87.2 (2)°; 87.9 (1)°, 89.4 (1)°; 89.3 (2)°; and 87.6 (1)° respectively for the Cu(II), Cu(I), Co(II), and Ni(II) complexes. Increasing *D*_{2d} flattening is reflected by the successive decrease in the interligand DA's observed for Cu(I) [76.8 (1)–78.9 (1)°], Co(II) [74.0 (2)°, 74.7 (2)°], Ni(II) [65.4 (2)°, 67.7 (2)°], and Cu(II) [51.1 (2)–54.2 (2)°]. The Cu(II)–N distances (Figure 1) are ca. 0.05 Å shorter than those generally observed for planar or tetragonal tetrakis(imidazole)copper(II) complexes⁵ but are typical for tetrahedrally distorted Cu(II) complexes having four sp² N-donors.^{10–12} The Cu(I)–N distances (Figure 2) are normal.^{15–18} The Co(II)–N distances [1.987 (4), 2.001 (6) Å] are the same as those [1.988 (3), 2.002 (3) Å] for the essentially tetrahedral (1,2-dimethylimidazole)₄Co·2ClO₄ complex.³⁰ The

Ni(II)–N distances [1.960 (5), 1.966 (6) Å] are similar to those of pseudotetrahedral Ni(II) tropocoronand complexes with DA's in the range 70.1–85.2°.¹⁴

Electronic spectra of the Cu(II) complex (mulls and solution) include a LF absorption at 660 nm (ε ~400) and the predicted³¹ π(imidazole) → Cu(II) LMCT absorption at 450 nm (ε ~600). The Cu(II)-doped Zn(II) complex exhibits axial EPR spectra (*g*_z = 2.32, *g*_⊥ = 2.06, *A*_{||}^{Cu} = 118 × 10⁻⁴ cm⁻¹) considerably different from those (*g*_{||} = 2.26, *g*_⊥ = 2.08, *A*_{||}^{Cu} = 178 × 10⁻⁴ cm⁻¹) of a planar tetrakis(phenylimidazole)copper(II) reference complex³² but similar to those³ for superoxide dismutase with Cu(II) doped into the Zn(II) site (*g*_z = 2.316, *g*_y = 2.118, *g*_x ≈ 2.01, *A*_z^{Cu} = 116 × 10⁻⁴ cm⁻¹). The Ni(II) complex exhibits LF absorptions at 770 (ε ~30), 640 (ε ~85), and 470 nm (ε ~140); the π(imidazole) → Ni(II) LMCT absorption appears at 350 nm (ε ~800). π(Imidazole) → Ni(II) LMCT at 335 and 355 nm has been reported for Ni(II)-substituted stellacyanin and azurin, respectively.⁶ The Co(II) complex exhibits LF absorptions at 590 (ε ~600) and 520 nm (ε ~470); the π(imidazole) → Co(II) LMCT absorption appears at 310 nm (ε ~900). The ligand **1** does not exhibit electronic absorptions at wavelengths longer than 300 nm.

Acknowledgment. This research was supported by the NSF (Grant CHE8417548), the David and Joanna Busch Foundation, and the NIH (Instrumentation Grant 1510 RRO 1486 O1A).

Supplementary Material Available: Full details for the synthesis of **1** and positional and thermal parameters for Cu(1)₂·2ClO₄, Cu(1)₂·ClO₄, Ni(1)₂·2ClO₄·3EtOH, and Co(1)₂·ClO₄·3EtOH (26 pages). Ordering information is given on any current masthead page.

(32) Prochaska, H. J.; Schwindinger, W. F.; Schwartz, M.; Burk, M. J.; Bernarducci, E.; Lalancette, R. A.; Potenza, J. A.; Schugar, H. J. *J. Am. Chem. Soc.* **1981**, *103*, 3446.

Reactivity of Pentaammineosmium(II) with Benzene

W. D. Harman and H. Taube*

Department of Chemistry, Stanford University
Stanford, California 94305
Received October 30, 1986

Our continued interest in the reactivity of pentaammineosmium(II) with unsaturated ligands^{1,2} has prompted us to investigate its interaction with unsubstituted aromatic hydrocarbons. When Os(NH₃)₅(CF₃SO₃)₃³ is reduced by magnesium in the presence of excess benzene, a deep orange solution results.^{4a} The material isolated from this reaction was characterized as [Os(NH₃)₅(η²-benzene)](TFMS)₂ (**1**).^{5a} The ¹H NMR spectrum of **1** at room temperature shows resonances at 4.75 and 3.45 ppm,

(1) Harman, W. D.; Fairlie, D. P.; Taube, H. *J. Am. Chem. Soc.* **1986**, *108*, 8223–8227.

(2) Taube, H. *Pure Appl. Chem.* **1979**, *51*, 901–912.

(3) Lay, P.; Magnuson, R.; Sen, J.; Taube, H. *J. Am. Chem. Soc.* **1982**, *104*, 7658.

(4) (a) Preparation of **1**: 200 mg of Os(NH₃)₅(TFMS)₃ and 1.0 mL of benzene are dissolved in a cosolvent mixture of 1.5 mL of dimethylacetamide (DMA) and 20 mL of freshly distilled dimethoxyethane. Magnesium, 1.0 g, cleaned with iodine and washed with DMA, is added and the stirred solution becomes orange. After 50 min, the reduced solution is filtered and treated with 100 mL of CH₂Cl₂, precipitating the final product. (b) Preparation of **2**: 1, 100 mg, is suspended in ethyl acetate (EtOAc) for 24 h. The solution is filtered and the precipitate collected and washed with EtOAc and Et₂O. **2** is recrystallized by vapor diffusion of ether into acetone.

(5) (a) **1**: Anal. Calcd for C₈H₂₁Os₁S₂F₆O₈N₅: C, 14.75; H, 3.25; N, 10.75. Found: C, 14.75; H, 3.48; N, 10.57. IR (KBr) 3040, 2961, 1529, 1450, 988, 927 cm⁻¹ (plus CF₃SO₃⁻ and ammine absorptions); ¹H NMR (acetone-*d*₆, 20 °C) δ 6.45 (5.5 H, br), 4.75 (3 H, br), 3.45 (12 H, br), -87 °C: 7.25 (2 H, br), 6.55 (2 H, br), 5.22 (2 H, br). (b) **2**: Anal. Calcd for C₈H₃₆Os₁S₂F₁₂O₁₂N₁₀: C, 11.76; H, 3.20; N, 10.94. Found: C, 11.60; H, 3.22; N, 11.04. IR (KBr) 3005, 2958 (m), 1464, 1156, 1047, 927 cm⁻¹ (plus SO₃CF₃⁻ and ammine absorptions); ¹H NMR (acetone-*d*₆) δ 6.53 (1.9 H, m), 4.63 (2.0, d), 4.33 (1.9, m), 4.90 (5.8, br), 3.65 (23, br); ¹³C NMR (acetone-*d*₆, proton decoupled) 127.6 (s), 53.1 (s), 49.6 (s), 123 (q) ppm (CF₃SO₃⁻).

(27) Hughey, J. L., IV; Knapp, S.; Schugar, H. J. *Synthesis* **1980**, 489.

(28) See the supplementary material for more information.

(29) Crystallography: Cu(1)₂·ClO₄, CuClO₄N₈C₃₆H₂₈, monoclinic, *C2/c*, *a* = 20.922 (7) Å, *b* = 20.603 (3) Å, *c* = 16.127 (3) Å, β = 90.36 (2)°, *Z* = 8; *d*_{obsd} = 1.40 (1), *d*_{calcd} = 1.406 g/cm³. The structure was solved (2252 reflections (*I* > 1σ(*I*)), Mo Kα radiation, 0.71073 Å, empirical absorption corrections) using the Enraf-Nonius SDP and refined to give *R*_{F(w_F)} = 0.070 (0.070) and a goodness of fit of 1.93. Cu(1)₂·2ClO₄, CuCl₂O₈N₈C₃₆H₂₈, orthorhombic, *Pbcn*, *a* = 17.581 (3) Å, *b* = 21.706 (2) Å, *c* = 19.154 (2) Å, *Z* = 8; *d*_{obsd} = 1.51 (1), *d*_{calcd} = 1.518 g/cm³, 2783 reflections (*I* > 1σ(*I*)), *R*_{F(w_F)} = 0.098 (0.095), and GOF = 2.24. Co(1)₂·2ClO₄·3EtOH, CoCl₂·O₁₁N₈C₄₂H₄₆, monoclinic, *C2/c*, *a* = 27.239 (4) Å, *b* = 13.041 (2) Å, *c* = 16.205 (2) Å, β = 125.39 (1)°, *Z* = 4; *d*_{obsd} = 1.41 (1), *d*_{calcd} = 1.371 g/cm³, 2019 reflections (*I* > 1σ(*I*)), *R*_{F(w_F)} = 0.070 (0.085), and GOF = 2.72. Ni(1)₂·2ClO₄·3EtOH, NiCl₂O₁₁N₈C₄₂H₄₆, monoclinic, *C2/c*, *a* = 26.842 (5) Å, *b* = 13.022 (2) Å, *c* = 16.406 (2) Å, β = 126.21 (1)°, *Z* = 4; *d*_{obsd} = 1.39 (1), *d*_{calcd} = 1.390 g/cm³, 2049 reflections (*I* > 3σ(*I*)), *R*_{F(w_F)} = 0.080 (0.085), and GOF = 2.25. The Co, Ni, and a nominally 3% Ni(II)-doped Zn(1)₂ complex (lattice constants *a* = 27.26 (1) Å, *b* = 13.021 (3) Å, *c* = 16.18 (1) Å, β = 125.44 (5)°) are isostructural. The perchlorate anions in all the complexes showed high thermal parameters and/or disorder, resulting in higher than normal *R* factors. Complete structural details will be presented elsewhere.

(30) Bernarducci, E.; Bharadwaj, P. K.; Potenza, J. A.; Schugar, H. J. *Acta Crystallogr. Sect. C*, accepted for publication.

(31) Bernarducci, E.; Schwindinger, W. F.; Hughey, J. L., IV; Krogh-Jespersen, K.; Schugar, H. J. *J. Am. Chem. Soc.* **1981**, *103*, 1686.

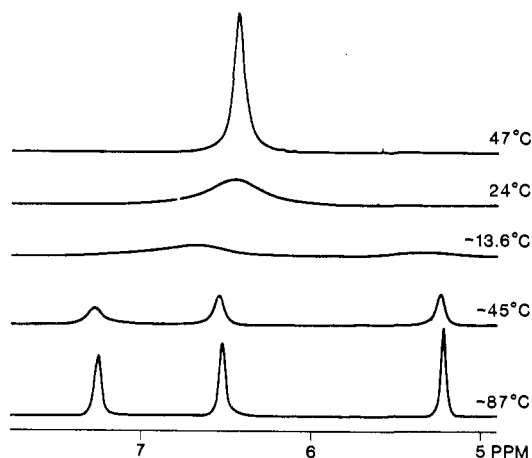
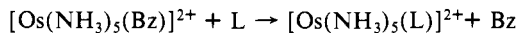


Figure 1. ^1H NMR of $[\text{Os}(\text{NH}_3)_5\text{Bz}](\text{TFMS})_2$ in acetone- d_6 with varying temperature.

corresponding to *trans*- and *cis*-ammines, and a very broad resonance at 6.45 ppm, indicating a fluxional benzene ligand. Lowering the temperature to -87°C (Figure 1) splits this broad peak into three well-defined peaks at 7.25, 6.55, and 5.22 ppm, confirming an η^2 -bound benzene. The IR spectrum of **1** shows absorptions at 3040 and 2961 cm^{-1} , indicating both olefinic and "aliphatic-like" C-H stretches. Though π -bound aromatic hydrocarbons are found in a wide variety of organometallic complexes, η^2 -bound aromatic molecules are uncommon. Of those reported, most are fluorinated or are stable only at low temperature.^{6a} Recently, Jones et al. have shown that an η^2 -bound arene is the intermediate for the C-H activation of benzene.^{6b} When a solution of **1** in acetone- d_6 is allowed to stand, benzene is liberated and the complex $[\text{Os}(\text{NH}_3)_5(\eta^2\text{-acetone})]^{2+}$ is formed. This reaction proceeds at room temperature with a half-life of about 8 h.⁷ We have found that **1** will react with a variety of ligands in the following general substitution reaction:⁸



where L = CH_3CN , $(\text{CH}_3)_2\text{CO}$ or isonicotinamide (isn).

If **1** is allowed to stand in an inert solvent for 24 h in the absence of a coordinating ligand, however, it will condense to give a binuclear complex $[(\text{Os}(\text{NH}_3)_5)_2(\mu\text{-}\eta^2\text{:}\eta^2\text{-benzene})]^{4+}$ (**2**).^{4b}

$[(\text{Os}(\text{NH}_3)_5)_2(\mu\text{-}\eta^2\text{:}\eta^2\text{-benzene})]^{4+}$. Even in the presence of excess benzene, **1** eventually will convert to the more stable binuclear complex **2**. Unlike its precursor, **2** is substitutionally inert, showing no reactivity in acetonitrile or acetone even after 36 h. The ^1H NMR spectrum of **2** shows three inequivalent benzene proton resonances per osmium pentaammine unit.^{5b} The decoupled ^{13}C NMR spectrum of **2** indicates three inequivalent carbon resonances at 127.6, 53.1, and 49.6 ppm. It is useful to compare these values with the ^{13}C resonances of ethylene,⁹ both as π -bound to Ni^0 (47.4 ppm) and as a free ligand (122.8 ppm). The comparison of these values suggests that **2** contains two types of carbon bound to osmium and one type of carbon which is still olefinic. The IR spectrum of **2** is very similar to that of **1**, showing absorptions both above and below 3000 cm^{-1} , indicating both olefinic and aliphatic-like C-H stretches. Inspection of a space-filling model of **2** indicates that the metal centers must reside on opposite sides of the benzene plane, and this together with the NMR data suggests the structure shown in Figure 2. Attempts to add a third $[\text{Os}(\text{NH}_3)_5]^{2+}$ unit have been unsuccessful, presumably due to the steric constraint.

(6) (a) Muetterties, E. L.; Blecke, J. R.; Wucherer, E. J.; Albright, T. A. *Chem. Rev.* **1982**, *82*, 499-525. (b) Jones, W. D.; Feher, F. J. *J. Am. Chem. Soc.* **1984**, *106*, 1650-1663. Also see: Sweet, J. R.; Graham, A. G. *J. Am. Chem. Soc.* **1983**, *105*, 305-306.

(7) The half-life is estimated on the basis of the formation of $[\text{Os}(\text{NH}_3)_5(\text{CH}_3)_2\text{CO}]^{2+}$ in the ^1H NMR,¹ assuming pseudo-first-order kinetics.

(8) The isn and CH_3CN substitution reactions were monitored by cyclic voltammetry.

(9) Tolman, C. A.; English, A. D.; Manzer, L. E. *Inorg. Chem.* **1975**, *15*, 2353.

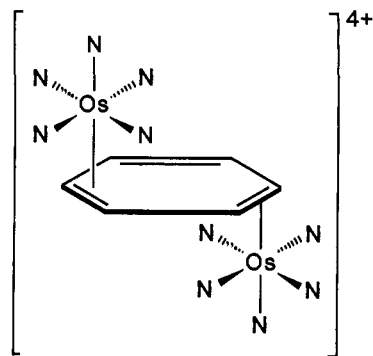


Figure 2. Proposed structure of $[(\text{Os}(\text{NH}_3)_5)_2\text{Bz}]^{4+}$.

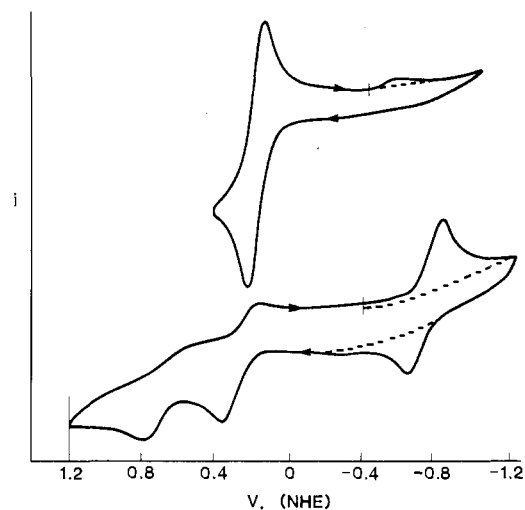


Figure 3. Cyclic voltammogram of $[(\text{Os}(\text{NH}_3)_5)_2\text{Bz}]^{4+}$ in DME with 0.5 N Na TFMS. $E_\gamma = 1.2, 0.5 \text{ V}; -1.2 \text{ V (NHE)}$; $\nu = 200 \text{ mV/s}$.

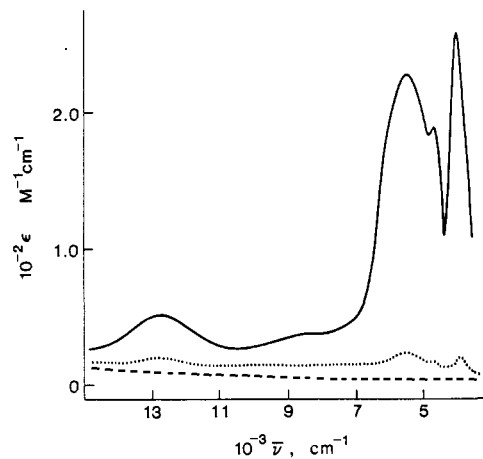


Figure 4. NIR absorption spectrum of $[(\text{Os}(\text{NH}_3)_5)_2\text{Bz}]^{5+}$ in acetone- d_6 : (---) **2** only; (—) **2** + $1[\text{Fe}(\text{Cp})_2]^+$; (···) **2** + $2[\text{Fe}(\text{Cp})_2]^+$.

van der Heijden et al. have recently published the crystal structure of a $\mu\text{-}\eta^2\text{:}\eta^2\text{-benzene}$ Re(I) binuclear complex, the ^1H and ^{13}C NMR spectra of which are in good agreement with the present work.¹⁰ To our knowledge the only other examples of η^2 -bound benzenes bridging more than one metal are for molecules in which benzene "caps" a metal cluster.¹¹

Electrochemistry. The cyclic voltammogram of **1** shows a chemically irreversible oxidation wave at +0.30 V (NHE) even at scan rates as high as 50 V/s.¹² The return scan yields a reduction wave at -0.75 V (NHE) which we ascribe to the re-

(10) van der Heijden, H.; Orpen, A. G.; Pasman, P. *J. Chem. Soc., Chem. Commun.* **1985**, 1576.

(11) Lewis, J., Et al. *J. Chem. Soc., Chem. Commun.* **1972**, 559.

(12) Electrochemical conditions: 0.5 N NaTFMS in DME. Au^0 working electrode; $[\text{Fe}(\text{Cp})_2]^+/\text{Fe}(\text{Cp})_2$ internal reference.

duction of $[\text{Os}(\text{NH}_3)_5(\text{DME})]^{3+}$. This is in contrast to the electrochemical behavior of $[\text{Os}(\text{NH}_3)_5(\text{ethylene})]^{2+}$, which shows reversible electrochemistry at scan rates as low as 50 mV/s.¹³ The cyclic voltammogram of **2** shows two oxidation waves at +0.35 and +0.85 V (NHE). Upon return scan there is a single wave at -0.75 V (NHE), indicating dissociation of the fully oxidized species. In contrast, if the switching potential is reset to +0.5 V, so that the potential remains negative of the second oxidation wave, the first oxidation at +0.35 V becomes reversible (see Figure 3), which shows that the mixed-valence complex is stable at least on the electrochemical time scale.

Figure 4 shows the near-IR absorption spectrum of a solution of **2** in neat acetone-*d*₆, with 1 equiv of $[\text{FeCp}_2]\text{PF}_6$ added and with 2 equiv of $[\text{FeCp}_2]\text{PF}_6$ added. The spectrum of the mixed-valence complex $[(\text{Os}(\text{NH}_3)_5)_2(\mu\text{-}\eta^2\text{-}\eta^2\text{-benzene})]^{5+}$ features a broad asymmetric absorption at 1750 nm (ϵ 220) with a width at half-maximum of 1600 cm^{-1} . Though this band is rather weak, its width is less than half of that calculated by the Hush model for a valence trapped system.¹⁴ This feature along with the large separation in potential of the first and second oxidation waves suggests that $[(\text{Os}(\text{NH}_3)_5)_2(\mu\text{-}\eta^2\text{-}\eta^2\text{-benzene})]^{5+}$ is a fully delocalized class III mixed-valence complex.¹⁵ Additional features at 2140 and 2460 nm are presumed to be spin-orbit transitions arising from the unpaired electron. The positions of these peaks, compared to those of typical Os(III) mononuclear complexes, are further indication of the delocalization in the binuclear complex.¹⁶

The high affinity of pentaammineosmium(II) for unsaturated ligands has been demonstrated in the case of dinitrogen,¹⁷ ketones,¹ aldehydes,¹⁸ and now aromatic hydrocarbons. In addition pentaammineosmium(II) appears to exhibit unusual reactivity toward both amides and esters. Our future efforts will be focused on the further development of this chemistry.

Acknowledgment. Support of this work by National Institutes of Health Grant GMI3638-21 and National Science Foundation Grant CHE85-11658 is gratefully acknowledged.

(13) Unpublished results; $E_{1/2} = 0.40$ V (NHE).

(14) Hush, N. S. *Prog. Inorg. Chem.* **1967**, *8*, 391.

(15) Creutz, C. *Prog. Inorg. Chem.* **1983**, *30*, 1.

(16) Lay, P. A.; Magnuson, R. H.; Taube, H., manuscript in preparation.

(17) Allen, A. D.; Senoff, C. V. *J. Chem. Soc., Chem. Commun.* **1965**, 621.

(18) Unpublished results.

Biosynthesis of Sesbanine. A Novel Origin for the Carbon Skeleton

Ronald J. Parry,* Robson Mafoti, and John M. Ostrander

Department of Chemistry, Rice University
Houston, Texas 77251

Received November 10, 1986

In 1979, Powell and co-workers isolated the unique alkaloid sesbanine (**1**) from cytotoxic seed extracts of *Sesbania drummondii* (Leguminosae).¹ Sesbanine initially appeared to exhibit marked inhibition in the P388 leukemia screen, but later studies showed that the highly purified compound is inactive.¹ The activity of *Sesbania* extracts was eventually traced to the presence of a structurally unrelated substance called sesbanamide.² Although sesbanine lacks apparent biological activity, the alkaloid still excites interest because of its unprecedented structure. This fact prompted us to pursue the biosynthetic investigations of sesbanine that will now be described.

The extremely low concentrations of sesbanine in *S. drummondii* seeds¹ made it necessary to carry out biosynthetic studies

(1) Powell, R. G.; Smith, C. R., Jr.; Weisleder, D.; Muthard, D. A.; Clardy, J. *J. Am. Chem. Soc.* **1979**, *101*, 2784. Powell, R. G.; Smith, C. R., Jr. *J. Nat. Prod.* **1981**, *44*, 86.

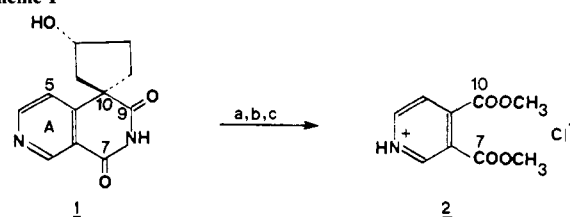
(2) Powell, R. G.; Smith, C. R., Jr.; Weisleder, D.; Matsumoto, G. K.; Clardy, J.; Kozlowski, J. *J. Am. Chem. Soc.* **1983**, *105*, 3739.

Table I. Administration of Labeled Precursors to *S. drummondii*^a

expt	precursor	% incorpn	labeling pattern
1	[carboxyl- ¹⁴ C]-nicotinic acid	0.002	68% in diester hydrochloride 2
2	[5- ³ H]-L-tryptophan	0.02	90% at C-5
	(sesbanine)	0.11	100% at C-5
	(nicotinic acid)		
3	[U- ¹⁴ C]-L-tyrosine	0.002	
4	[U- ¹⁴ C]-L-phenylalanine	0.007	
5	[G- ¹⁴ C]shikimic acid	0.025	17% in diester hydrochloride 2
6	[7- ¹⁴ C]shikimic acid	0.042	90% at C-9
7	[U- ¹⁴ C]- <i>p</i> -hydroxybenzoic acid	0.082	18% in diester hydrochloride 2 , 97% in oxindole 3 , 79% in phthalimidine 4

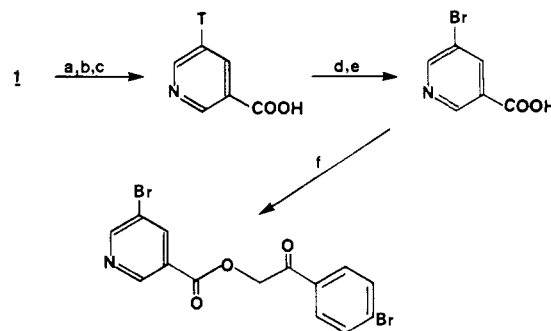
^a All precursors were administered to 6-week-old *Sesbania* plants by the cotton-wick method for a 7-day period.

Scheme I



^a KMnO_4 , KOH. ^b CH_2N_2 . ^c HCl.

Scheme II



^a PhCOCl , $\text{C}_5\text{H}_5\text{N}$. ^b KMnO_4 , KOH. ^c Δ . ^d SOCl_2 . ^e Br_2 . ^f *p*- $\text{BrPhCOCH}_2\text{Br}$, K_2CO_3 , crown ether.

using isotope dilution methods. The sesbanine required as carrier was obtained via total synthesis.³ The structure of sesbanine suggested that nicotinic acid might be a specific precursor. Accordingly, preliminary experiments were carried with [carboxyl-¹⁴C]nicotinic acid to optimize conditions for precursor incorporations. The best conditions gave an incorporation of 0.002% with this substance (Table I, experiment 1). The sesbanine biosynthesized from [carboxyl-¹⁴C]nicotinic acid in experiment 1 was degraded (Scheme I) to dimethyl pyridine-3,4-dicarboxylate hydrochloride (**2**), which carried 68% of the total radioactivity (theory = 100%). The low incorporation and relatively low specificity observed with nicotinic acid suggested that the plants may not efficiently utilize administered nicotinic acid. Therefore, tryptophan, which is a known nicotinic acid precursor in animals and some microorganisms,⁴ was evaluated as a sesbanine precursor. Administration of [5-³H]tryptophan to *Sesbania* was followed by workup with dilution for both sesbanine and nicotinic acid. The results of this experiment (Table I, experiment 2) were gratifying, since good incorporations into both substances were obtained. Furthermore, the tritium label in the isolated sesbanine and

(3) Kende, A. S.; Demuth, T. P. *Tetrahedron Lett.* **1980**, *21*, 715.